

John W. Cooper

University of Pennsylvania

Department of Physics

Philadelphia, Pennsylvania USA

Summary

Three papers on hadronic production of charmonium were submitted to this conference and are described briefly here. The Fermilab-Illinois-Pennsylvania-Purdue-Tufts collaboration [1] using the CYCLOPS spectrometer at Fermilab reported new results on  $\chi$  production by  $\pi^-$  and  $p$  at 200 GeV/c, showing the  $\chi(3510)$  and  $\chi(3555)$  produced with roughly equal cross sections in  $\pi^-$  collisions while the  $\chi(3555)$  dominates in  $p$  collisions. The IHEP-IIISN-LAPP collaboration [2] using the GAMS-2000 spectrometer at Serpukov reported the observation of inclusive  $\chi$  production in  $\pi^- p$  near threshold (38 GeV/c). The Annecy-CERN-Genova-Lyon-Oslo-Roma-Strasbourg-Torino collaboration [3] reported preliminary results on the direct formation of  $\eta_c$ ,  $\chi(3510)$ ,  $\chi(3555)$  in  $p\bar{p}$  collisions studied using a gas jet target in the ISR. Results on the related topic of upsilon production in  $\pi^- W$  interactions at 194 GeV/c were given in a fourth paper submitted by the CERN-Naples-Palaiseau-Strasbourg-Zürich collaboration (NA10) [4].

Differences Between Proton and  $\pi^-$  Induced Production of the Charmonium  $\chi$  States

Hadronic charmonium production was studied at Fermilab using a 190 GeV/c  $\pi^-$  beam and proton beams of 200 and 250 GeV/c to produce the  $\chi$  states in a beryllium target. The same apparatus was used in all cases to detect the decays  $\chi \rightarrow J/\psi + \gamma$  and  $J/\psi \rightarrow \mu^+ + \mu^-$  with resolution sufficient to unfold the three  $\chi$  states. The experimental apparatus was the superconducting Chicago Cyclotron Magnet Particle Spectrometer (CYCLOPS) facility, shown in Fig. 1. The event trigger favored the selection of high mass muon pairs. Muon tracks were reconstructed using data from a 24 plane multiwire proportional chamber system and a four plane drift chamber system. The resulting dimuon mass spectra for proton and  $\pi^-$  beams both show clean peaks at the  $J/\psi$  mass with a 22 MeV width ( $\sigma$ ) consistent with the expected resolution. Gaussian fits with polynomial backgrounds yielded  $157 \pm 17$  proton induced  $J/\psi$ 's and  $908 \pm 41$   $\pi^-$  induced  $J/\psi$ 's. Dimuons in the mass range 3.05 to 3.15 GeV were considered to be  $J/\psi$ 's and constrained to the known mass of 3.097 GeV.

The photon detector consisted of a lead glass calorimeter (21 radiation lengths thick) with a proportional tube array for position determination.

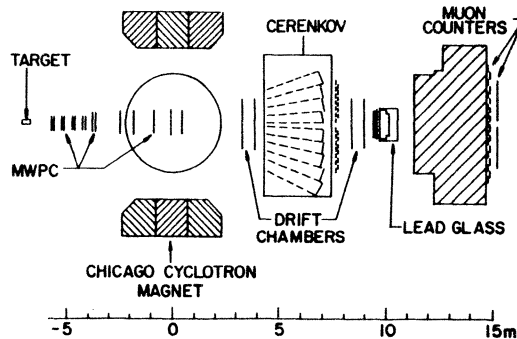
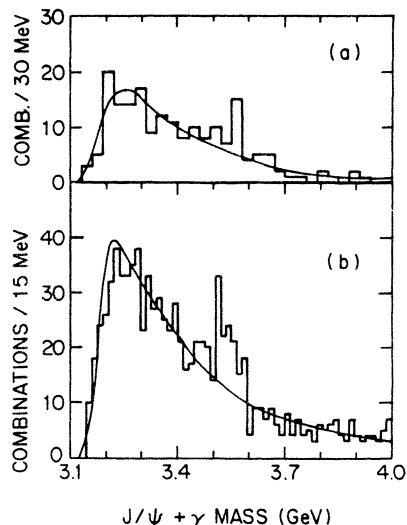


Figure 1. The CYCLOPS spectrometer.

Photons used in the analysis were required to be well isolated from other photon candidates and to have an energy between 3 and 50 GeV. Based on the clear observation of  $\pi^0$  and  $\eta$  signals at the correct masses, the photon energy scale is demonstrated to be accurate to the 1% level.

In Fig. 2, the  $J/\psi + \gamma$  mass spectra for incident proton and  $\pi^-$  beams are compared. The same apparatus and analysis were used for both data sets so that systematic differences should be negligible. The proton sample shows a significant excess of events in the  $\chi$  region which is narrower and at higher mass than the peak in  $\pi^-$  data. The superimposed background curves were calculated by combining photons from  $J/\psi$  events with  $J/\psi$ 's from other events. A small kinematic enhancement to this background due to the mixing of photons from  $\chi$  radiative decays with uncorrelated  $J/\psi$ 's was removed.

Figure 2.  $J/\psi + \gamma$  mass spectra for (a) proton and (b)  $\pi^-$  data in the CYCLOPS spectrometer.

In the  $\pi^-$  data the  $\chi(3510)$  and  $\chi(3555)$  states are not cleanly separated, but the width of the distribution is much broader than the expected 15 MeV ( $\sigma$ ) resolution and the peak is intermediate between the two  $\chi$  states. The number of  $\pi^-$  induced  $\chi$  events was determined in a fit to two gaussians to be  $53.6 \pm 17.1$ , with  $33.9 \pm 14.0$  in the lower mass peak and  $19.7 \pm 9.8$  in the higher mass peak. These numbers imply that the fraction of  $J/\psi$ 's produced via radiative decay in  $\pi^-$  interactions is  $0.31 \pm 0.10$ . Furthermore, using the known branching ratios for  $\chi \rightarrow J/\psi + \gamma$ , the cross section ratio  $\sigma(\chi(3510)) / \sigma(\chi(3555))$  is  $0.96 \pm 0.64$  for incident  $\pi^-$ . This experiment is in good agreement with previous  $\pi^-$  results [5-7].

The proton signal is stable against changes in analysis cuts and binning in spite of the limited statistics. A count of excess events above background in the mass regions 3.495-3.540 and 3.540-3.585 GeV which contain the  $\chi(3510)$  and  $\chi(3555)$  signals in the  $\pi^-$  data yields 3.5 events over a background of 9.5

events in the lower-mass region and 8.3 events over a background of 7.7 events in the higher-mass region. The total of  $11.8 \pm 5.4$  events implies that the fraction of  $J/\psi$ 's produced via radiative  $X$  decay is  $0.47 \pm 0.23$  for proton interactions. This agrees with one ISR experiment at higher energy [8] and disagrees with another [9]. However, this is the first experiment to measure proton  $X$  production with resolution sufficient to distinguish between  $X$  states. The ratio  $\sigma(X(3510)) / \sigma(X(3555))$  is measured to be  $0.24 \pm 0.28$  for incident protons and is much lower than the ratio in  $\pi^-$  interactions. This dominance of the  $X(3555)$  suggests [10] that simple gluon fusion is sufficient to account for the bulk of  $X$  production in proton interactions. This contrasts with the more complicated situation for  $\pi^-$  collisions where other mechanisms are clearly important.

#### $X$ Particle Production in $\pi^- p$ Collisions at 38 GeV/c

These measurements were performed with 38 GeV/c  $\pi^-$  produced by the 70 GeV synchrotron at IHEP.  $X$  particles were identified through their decay into  $J/\psi + \gamma$  and the  $J/\psi$  particles by their decay into  $e^+ e^-$ . Photon and electrons (positrons) were detected in the hodoscope spectrometer GAMS-2000, a matrix of  $48 \times 32$  lead-glass counters.

Events were selected with electron showers of energy  $> 7$  GeV, with an electron pair energy  $> 21$  GeV, and charged particle multiplicity  $\leq 7$ . The resulting  $e^+ e^-$  effective mass spectrum contains 120 events with a mass  $> 2.3$  GeV and shows clean  $J/\psi$  peak of 40 events. The distribution of selected  $J/\psi$ 's versus  $x_F$  has a sharp drop for  $x_F < 0.4$  due to the acceptance of the spectrometer and to the analysis cuts.

Events were then selected with an electron pair in the mass range 3.0-3.3 GeV and an isolated photon with energy  $> 2$  GeV. The mass of the selected  $e^+ e^-$  events was evaluated fixing the  $J/\psi$  mass to its known value and the resulting mass spectrum is shown in Fig. 3. A peak corresponding to  $X$  particles is seen near 3.5 GeV with no visible background and a width close to the resolution of the spectrometer. The fraction of  $J/\psi$ 's produced via radiative decay is found to be  $0.44 \pm 0.16$ .

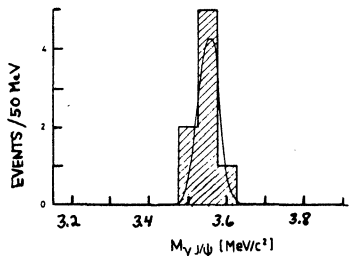


Figure 3.  $J/\psi + \gamma$  mass spectrum from GAMS-2000.

#### Formation of Charmonium States in $\bar{p}p$ Annihilation

The  $\bar{p}p$  channel allows the formation study of  $cc$  states not directly accessible in the  $e^+ e^-$  annihilation channel. Until now this very interesting property was offset by the difficulty of designing a source comparable in luminosity and energy definition to the one provided by an  $e^+ e^-$  collider. The intense  $\bar{p}$  beam now available at CERN with the A.A. facility and their precise momentum definition obtained with the stochastic cooling system have made these experiments feasible.

The  $\bar{p}$  beam was injected in ring 2 of ISR, and the beam momentum was tuned in such a way that the c.o.m. energy was in the region of the mass of the resonance to be studied. The excitation curve was constructed by changing the beam momentum in steps, and at each step the number of events for the selected decay channel was determined. An internal gas jet target provided the protons for collisions. The detector was a two-arm non-magnetic lead glass spectrometer complemented by a large-acceptance lead scintillator sandwich veto system and a silicon detector telescope to monitor the source luminosity. The  $J/\psi$ ,  $X$ ,  $\eta_c$  were detected through the decays  $e^+ e^-$ ,  $\psi\gamma$ ,  $\gamma\gamma$ , respectively. The absolute energy calibration of the ISR was accomplished through formation of the  $J/\psi$ , whose mass is known to  $\pm 100$  keV.

The excitation curves for  $X(3510)$  and  $X(3555)$  are given in Fig. 4. The preliminary results for the masses and partial widths to  $\bar{p}p$  are:

$$M_1 = 3511.4 \pm .3 \pm .4 \text{ MeV}, \Gamma_{\bar{p}p} = 62 \pm 15 \text{ eV},$$

$$M_2 = 3556.8 \pm .4 \pm .4 \text{ MeV}, \Gamma_{\bar{p}p} = 208 \pm 75 \text{ eV}.$$

An energy scan in the  $\eta_c$ -region, coupled with the MARK III results on the  $\eta_c \rightarrow \bar{p}p$  branching ratio yields:

$$BR(\eta_c \rightarrow \gamma\gamma) = (2.4 \pm 2.0) \cdot 10^{-4}, \Gamma_{\gamma\gamma} = 2.7 \pm 2.3 \text{ keV}.$$

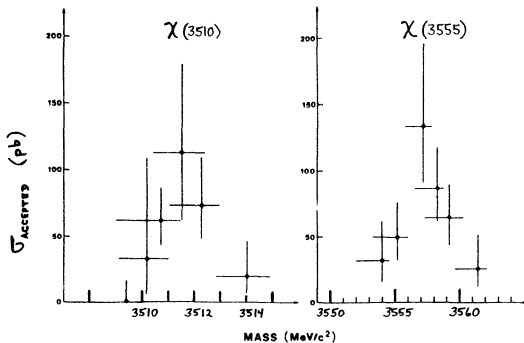


Figure 4.  $X(3510)$  and  $X(3555)$  excitation at the ISR.

#### Upsilon Production at CERN

Upsilon family production was observed at the SPS by the NA10 group in  $\pi^- W$  collisions at 194 GeV/c. They fit a sample of 2000 upsilon family events to three gaussians and obtain the ratio  $(T' + TT') / T = 0.53 \pm 0.19$ . Assuming a linear  $A$  dependence they find  $B_{\mu\mu} \sigma = 1.04 \pm 0.05 \text{ stat} \pm 0.19 \text{ sys} \text{ pb/nucleon}$ .

#### References

1. J.W. Cooper *et al.*, paper No. 616.
2. F. Binon *et al.*, paper No. 488, CERN-EP/84-13.
3. C. Baglin *et al.*, paper No. 533.
4. B. Beter *et al.*, paper No. 429.
5. T.B.W. Kirk *et al.*, Phys. Rev. Lett. **42**, 619 (1979).
6. S.R. Hahn *et al.*, to be published in Phys. Rev. D.
7. Y. Lemoigne *et al.*, Phys. Lett. **113B**, 509 (1982).
8. C. Kourkoumelis *et al.*, Phys. Lett. **81B**, 405 (1979).
9. A.G. Clark *et al.*, Nucl. Phys. **B142**, 29 (1978).
10. C.E. Carlson and R. Suaya, Phys. Rev. **D18**, 760 (1978).

SUBRAMANIAN, A.

Tata Institute of Fundamental Research  
Bombay 400005, India

We would like to see the level of inclusive cross-section in hadroproduction of charm ( $\sigma_{cc}$ ) determined to a precision  $< 10\%$  from fixed target experiments. The ordinary manifestations of  $c\bar{c}$  are  $D\bar{D}$  (including  $D^*$ 's),  $\Lambda_c^+\bar{D}$  and  $F^+X$  in commonly available  $\pi$ -p(N) and p-p(N) collisions at incident energies  $E_{inc} \gtrsim 100$  GeV. One would like to obtain the dependence of the cross-sections on  $E_{inc}$  and study the  $x_F$ ,  $p_T$  and nuclear target A dependences. One would also be interested in the charm pair mass ( $M_{cc}$ ) distributions at production and the kinematic correlations between associated partners of charm.

Three different techniques that have been employed in the above studies can be classified as (a) direct (Vertexology), (b) semi-direct (Peakology) and (c) indirect (inclusivology). In (a), high resolution vertex detectors are needed to locate the decay vertices of short lived ( $\sim 10^{-13}$  sec) particles. In (b), the charm decays are not separately identified but estimated from the kinematic mass peaks seen in certain decay channels (like  $D^+ \rightarrow K^+ \pi^+ \pi^-$ ) and suffer from combinatorial background due to particles at the production vertex. Here one has to enrich the signal by identifying either a lepton ( $e, \mu$ ) or a kaon from the production vertex. Examples of method (c) are the studies on beam dump neutrino's or other prompt lepton production studies which need extra inputs like  $x_F$ ,  $p_T$  and A dependences to deduce an inclusive charm cross-section. The clearest experiments are the ones belonging to (a) equipped with good momentum spectrometer and particle identification devices downstream. Only then kinematic ambiguities in fitting the decay vertices like 3 prongs with  $D/\Lambda_c^+$  hypotheses can be minimized.

Systematic uncertainties have to be kept below 10% level which seem difficult in view of various acceptance and detection efficiency estimations, kinematic ambiguities etc. apart from uncertainties in the input decay branching ratios. The LEBC-EHS Collaboration [1] suggested that some of the hadronic decay branchings taken over from the early SPEAR results [2] would need upward revision and Mark III data reported at this Conference [3] have in fact

indicated an increase by about a factor of two. This leads to a down-ward revision of many of the hadroproduction estimates of inclusive charm cross-sections by this factor. It also reduces some of the self inconsistencies in the ISR data [4].

The level of hadroproduced charm  $D\bar{D}$  currently indicated at CERN SPS energies is  $\gtrsim 20 \mu b$ . At ISR energies,  $\sigma_{D\bar{D}} \gtrsim 200 \mu b$ . This rise, which could be even more spectacular for  $\Lambda_c^+\bar{D}$  production, would be investigated in a new experiment at Fermilab (E-743) using the LEBC transported from CERN. Reliable estimates of  $\Lambda_c^+\bar{D}$  and  $F^+$  production have yet to be obtained at SPS energies.

In view of various systematics involved in the evaluation of charm cross-sections, some self consistency checks are useful like the Fischer-Geist type of limits [5,6]. However, these limits are dependent on the  $M_{cc}$  distribution assumed as pointed out by Ganguli et al. in a paper to this Conference (No. 124, B10).

The A dependence of charm production seems linear comparing different vertexological data [7]. The FFMOW measurement [8] on prompt neutrinos has given a proportionality like  $A^{0.72}$ . This raises all previous inclusivological estimates of  $D\bar{D}$  cross-sections by factors 3-4 and a new disagreement with vertexological results appears. Such a discrepancy could be interpreted as an indicator of a new non-charm source of prompt neutrino (muon?) production [9]. Due to these interesting issues, there are strong reasons to pursue the goals stated in the beginning.

REFERENCES

1. M. Aguilar-Benitez et al., Phys. Lett. 135B (1984)
2. G.H. Trilling, Phys. Rep. 75 (1981) 57.
3. R. Schindler, Talk at this conference, Session B10.
4. A. Putzer, Proc. of the Int. Europhys. Conf. on HEP, Brighton, 1983, p. 308.
5. H.G. Fischer and W. Geist, Z. Phys. C19(1983)159.
6. J. Badier et al., Phys. Lett. 142B (1984) 446.
7. S. Tavernier, Talk at this Conference, Session B10.
8. R.C. Ball et al., Preprint UM HE 83-16, August 1983.
9. A. Subramanian, Paper No. 313 to this Conference, Session B10.

**H. Wachsmuth**  
**CERN - European Organization for Nuclear Research**  
**EP Division**  
**1211 GENEVA 23, Switzerland**

### **1. INTRODUCTION**

One of the purposes of beam dump experiments is to search for the production of short-lived ( $T < 10^{-11}$ s) particles in hadron-hadron collisions, which decay into neutrinos (called prompt neutrinos), like charmed particles, heavy leptons etc. The 1982 CERN Beam Dump experiments were mainly done to check - with an improved layout and more statistics - possible anomalies in the results of previous beam dump experiments, especially a possible non-equality of prompt  $\nu_e$  and  $\nu_\mu$  fluxes.

### **2. METHOD**

400 GeV protons were transported through vacuum ( $< 0.03$  T) monitored against beam losses ( $< 10^{-5}$ ), and dumped into blocks of copper of full ( $\sim 2/3$  of the time) and 1/3 density ( $\sim 1/3$  of the time). In these dumps nearly all conventional hadrons ( $\pi$ ,  $K$ ,  $\Lambda$ , ...) making neutrinos (called conventional neutrinos) are absorbed. Three neutrino detectors: BEBC (11.5 t of  $\text{Ne}/\text{H}_2$  mixture, an excellent electron identifier, surrounded by absorber and wire chambers serving as a muon identifier), CDHSW ( $\sim 450$  t of mainly steel, scintillators and drift chambers, an excellent muon identifier), and CHARM ( $\sim 90$  t of mainly marble, scintillators and wire chambers), respectively 406, 465 and 487 m downstream of the dump, behind a shield of 180 m steel and 170 m earth and rock, recorded neutrino interactions. Prompt neutrino event rates were derived from the total event rates either by extrapolating the rates taken with full and 1/3 density dumps to infinite density (CDHSW), or by subtracting the conventional neutrino event rate determined via the muon fluxes measured in the shielding (BEBBC), or using both procedures (CHARM and - to some extent - BEBBC).

### **2. EVENT RATES**

Event rates due to prompt neutrinos above 20 GeV neutrino energy, per ton of fiducial detector mass and  $10^{18}$  protons on dump are given in table 1. They are multiplied by solid angle factors weighted for neutrino spectrum and cross section,  $f_\Omega$  (statistical error quoted first, for BEBBC statistical and systematic errors - typically in the ratio 2 : 1 - are added in quadrature).

These rates are nearly final apart from small corrections still being worked on. The rates for CHARM are based on those quoted earlier [1].

The prompt  $\nu_e$  and  $\nu_\mu$  fluxes can be compared by calculating the  $e-\mu$ -asymmetry  $A = (\nu_e^+ - \nu_\mu^+)/(\nu_e^+ + \nu_\mu^+)$ , which is  $0.26 \pm 0.15$ ,  $-0.07 \pm 0.12$ ,  $-0.32 \pm 0.08$  from the three detectors, respectively. Only the CHARM value seems to differ significantly from zero, caused by the large prompt muon rate (table 1).

The ratio of  $e^+$  to  $e^-$  rates observed in BEBBC ( $0.21 \pm 0.06$ ) differs significantly from the total cross section ratio  $\sigma^V/\sigma^V = 0.47 \pm 0.02$ , indicating associated production of fast charmed baryons and slow charmed anti-mesons at the source of prompt neutrinos. The corresponding value from CDHSW ( $\mu^+/\mu^- = 0.34 \pm 0.11$ ) is consistent with  $\sigma^V/\sigma^V$ , but also with the BEBBC result.

### **3. CHARM PRODUCTION CROSS SECTIONS**

The observed prompt  $\nu_e$  and  $\nu_\mu$  fluxes are attributed to charm production in pCu collisions with subsequent semi-leptonic decay. The neutrino detectors (which historically were the first ones to establish this process) are sensitive to charmed particles produced only at large  $x$  ( $= P_{\text{charm}}/P_{\text{proton}}$ -values). Although these forward produced rates are well measurable (to better than 20%), total production rates depend strongly on production models assumed. Moreover, the particles are produced in dense material (copper). Hence, assumptions have to be made about the dependence of the production cross section on energy, the probabilities for proton re-interactions (cascade effect), of intranuclear charmed particle absorption, and about semileptonic decay type and branching ratio which are not yet well established. Also the dependence of the production cross section on the mass number  $A$  over the whole  $x$  range is still under discussion [2].

Since the three experiments agree within errors about the  $\nu_e$  production rate, charmed particle production cross sections based on electron event rates will be the same if similar assumptions are

**TABLE 1**

Final state lepton	BEBBC ( $f_\Omega = .76$ )	CDHSW ( $f_\Omega = 1.0$ )	CHARM ( $f_\Omega = 1.10$ )
$\mu^-$	$1.5 \pm .7$	$2.5 \pm .4 \pm .3$	
$\mu^+$	$.9 \pm .2$	$.9 \pm .2 \pm .1$	
$\mu^- + \mu^+$	$2.4 \pm .8$	$3.48 \pm .43 \pm .38$	$7.59 \pm .84 \pm .61$
$e^-$	$3.3 \pm .4$		
$e^+$	$.7 \pm .2$		
$e^- + e^+$	$4.00 \pm .40$ <sup>(a)</sup>	$3.05 \pm .24 \pm .44$ <sup>(b)</sup>	$3.80 \pm .68 \pm .29$ <sup>(a)</sup> $3.87 \pm .28 \pm .19$ <sup>(b)</sup>

(a) electrons identified

(b) by subtracting neutral current rates from muonless event rates

(\*) Based on papers by H. Wachsmuth (BEBBC), J. Duda (CDHSW) and discussion remarks by F. Niebergall (CHARM) in session B10 at XXII High-Energy Physics Conference, Leipzig, 18-25 July 1984.

made. Using the prompt electron event rate observed in BEBC, which is within errors the same as in the 1979 layout when scaled to the new distance from the dump (406 vs 821 m) and making the same assumptions about production (only  $D\bar{D}$ ,  $\sigma \sim A^1(1-x)^n e^{2pt}$ ,  $n = 4$ ), the same  $\sigma \cdot BR$ -value will be obtained: 1.2  $\mu b/\text{nucleon}$ . Assuming equal  $D^\pm$  and  $D^0$  production and the average semileptonic branching ratio [3],  $BR = (12 \pm 3)\%$ , the total charm production cross section will be 10 or 31  $\mu b/\text{nucleon}$  for  $\sigma \sim A^1$  or  $A^{0.72}$ , resp., with 10% error due to event rate, 25% error due to  $BR$ , and a large error due to production model uncertainties ( $\pm 70\%$  for  $\Delta n = \pm 1$  [4]). It should also be noted that the  $e^+/e^-$  ratio observed in BEBC indicates other production mechanisms than only  $D\bar{D}$  production, e.g.  $\Lambda_c \bar{D}$  with fast  $\Lambda_c$  and slow  $\bar{D}$  [5].

#### 4. CONCLUSION

The three CERN beam dump experiments have nearly final results from their 1982 data establishing clearly the existence of prompt  $\nu_e$ ,  $\bar{\nu}_e$ ,  $\nu_\mu$  and  $\bar{\nu}_\mu$  fluxes. BEBC and CDHSW are consistent with  $\mu$ - $e$  universality. All three experiments agree in the  $e^\pm$  event rate yielding production cross sections for charmed particles in the 10-40  $\mu b/\text{nucleon}$  range depending on assumptions. The  $e^+/e^-$  ratio observed in BEBC (consistent with the  $\mu^+/\mu^-$  ratio observed in CDHSW) favours associated production of a fast charmed baryon and a slow charmed anti-meson.

#### REFERENCE

- [1] A. Capone, Proceedings of the Europhys. Conf. on High Energy Physics (1983) 312.
- [2] S. Tavernier, contribution to this conference.
- [3] Particle Data Group, Rev. Mod. Phys. 56(2) (1984) 513.
- [4] H. Wachsmuth, Proceedings of the Topical Conf. on Neutrino Physics at Accelerators, Oxford 1978, RL-78-081.
- [5] G. Ringland and H. Wachsmuth, Univ. of Wisconsin Report, COO 088-116 (80 PI 328).

# MEASUREMENT OF THE TOTAL CHARM PRODUCTION CROSS SECTION IN 350 GeV p-Fe INTERACTIONS

Presented by Arie Bodek  
University of Rochester, Rochester, N. Y. 14627 USA

A. Bodek,<sup>1</sup> R. Breedon,<sup>1</sup> R.N. Coleman,<sup>1</sup> W. Marsh,<sup>1</sup> S.L. Olsen,<sup>1</sup> J.L. Ritchie,<sup>1</sup> I.E. Stockdale,<sup>1</sup> B.C. Barish,<sup>2</sup>  
R.L. Messner,<sup>2</sup> M.H. Shaevitz,<sup>2</sup> E.J. Siskind,<sup>2</sup> F.S. Merritt,<sup>3</sup> H.E. Fisk,<sup>4</sup> Y. Fukushima,<sup>4</sup> P.A. Rapidis,<sup>4</sup>  
G. Donaldson,<sup>5</sup> S.G. Wojcicki<sup>5</sup>

Rochester<sup>1</sup> - Caltech<sup>2</sup> - Chicago<sup>3</sup> - Fermilab<sup>4</sup> - Stanford<sup>5</sup>

## INTRODUCTION

We have measured the distribution of prompt single muons produced in 350 GeV p-Fe and 278 GeV  $\pi^+$ -Fe interactions. Prompt single muons originate from the production and semileptonic decays of charm states. A  $P_\mu > 9$  (GeV/c) trigger accepts almost all semileptonic decays of charm states produced with Feynman  $X_F > 0$ , as shown in Fig. 1a. Such data yield an almost model independent determination of the total charm production cross section (for  $X_F > 0$ ), and provide information on the  $X_F$  and transverse momenta ( $P_\mu$ ) distributions of hadrohically produced charm states.

## THE EXPERIMENT

Data were taken with both 350 GeV protons and 278 GeV pions incident on a variable density iron-scint. calorimeter. Single muons and dimuons were identified in a large acceptance iron-scintillator muon range detector interspersed with spark chambers, and in a toroidal iron magnetic spectrometer. The prompt single muon rates were extracted using the variable target density technique. Data were taken at low intensity with the  $P_\mu > 9$  (GeV/c) range trigger, and at high intensity with a forward  $P > 20$  (GeV/c) trigger. The results from the  $P > 20$  (GeV/c) data have already been published<sup>1,2</sup>. These include limits on  $D^0$ - $\bar{D}$  mixing, and limits on intrinsic charm. The forward prompt single muon distributions were also used to extract  $D$  meson production distributions<sup>2</sup> for  $X_F > 0.2$ . Fits of the form

$$E_D \frac{d^3 \sigma_D}{dp^3} \propto (1 - X_F)^n e^{-bP_\mu} t \quad (1)$$

yield  $n = 5.0 \pm 0.8$  and  $b = 2.0 \pm 0.3$  for 350 GeV p-Fe interactions. Extrapolation of such fits to  $X_F = 0$  yield<sup>2</sup>

$$\begin{aligned} p\text{-Fe: } \sigma_D &= 10.7 \pm 1.1 (\pm 1.8) (X_F > 0) \text{ } \mu\text{b/nucleon} \\ \pi^+\text{-Fe: } \sigma_D &= 17.5 \pm 5.5 (X_F > 0) \text{ } \mu\text{b/nucleon,} \end{aligned}$$

where the first error is statistical and the second error (for 350 GeV protons) results from the uncertainty in the exponent  $n$ . These cross sections were extracted assuming a linear  $A$  dependence of the total production cross section, an average semileptonic branching ratio of 8% for charm states, and under the assumption that the form of equation (1) holds for  $X_F < 0.2$ . The analysis of the recently analyzed  $P_\mu > 9$  (GeV/c) data does not require this latter assumption.

## RANGE ( $P_\mu > 9$ (GeV/c)) TRIGGER RESULTS

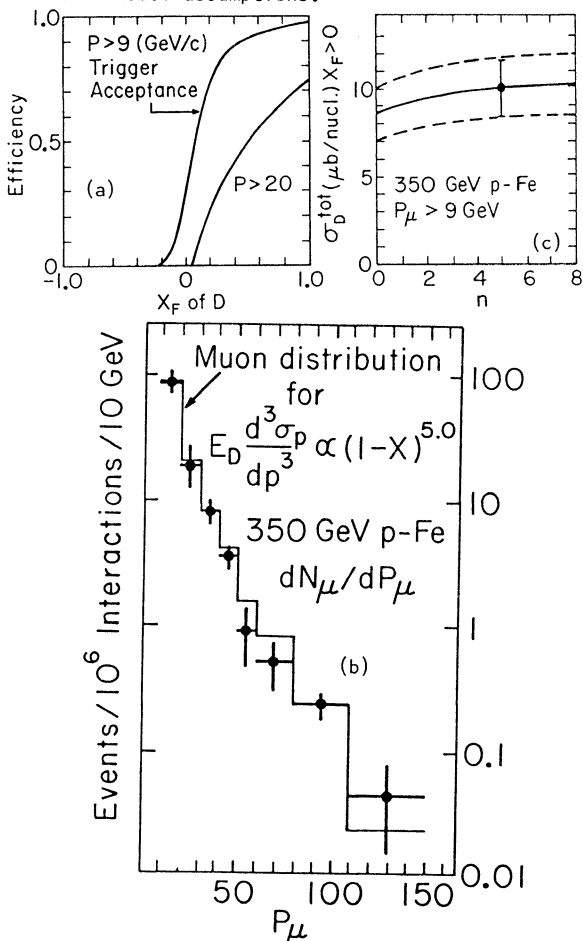
The momentum distributions for prompt single muons produced in 350 GeV p-Fe interactions are shown in figure 1(b). The range trigger data and the forward trigger data were combined in the analysis. Shown are the geometrical-acceptance-corrected rates  $dN_\mu/dP_\mu = dN_\mu^+/dP_\mu + dN_\mu^-/dP_\mu$  per inelastic proton interaction. The solid curve is the expected curve if  $D$  mesons are produced with a  $(1-X_F)^5$  distribution, which provides a good description of the data. Figure 1(c) shows the values of the extracted total charm production cross section per nucleon ( $X_F > 0$ ) under various assumptions for the exponent  $n$ . The extracted value of  $10 \pm 2 \mu\text{b/nucleon}$  for  $n = 5$  is rather insensitive to the  $X$ -dependence of  $D$  meson production. This cross section is for charm production in the primary p-Fe interaction. About 30% of the prompt muon rate is due to charm production from secondary interactions in the target calorimeter.

A comparison of this model independent cross section on iron with the cross section of  $14^{+6}_{-3} \mu\text{b/nucleon}$  obtained in 360 GeV p-p collisions in the LBC hydrogen filled bubble chamber<sup>3</sup> indicates that the  $A$ -dependence of the total charm production cross section is close to  $A^1$ . The hydrogen data also imply

$dN_D/dX_F \propto (1-X_F)^{1.8 \pm 0.8}$  which is flatter than what is indicated by our data. This difference may be due to a distortion of the  $X$  distributions from nuclear effects as predicted in some theoretical charm production models<sup>4</sup>. Note however, that the  $A$ -dependence of the total charm production cross section, within such models, is expected to be linear since it is dominated by production near  $X_F = 0$ .

1. A. Bodek et.al. Phys. Lett. 113B(1982)77,82.
2. J. L. Ritchie et.al. Phys. Lett. 126B(1983)499; 138B(1984)213; Phys. Rev. Lett. 44,230(1980); J. L. Ritchie, Ph.D. Thesis, Rochester 1984 available as UR861 (1984).
3. M. Aguilar-Benitez et.al. Phys. Lett. 123B(1983), 103; see also these proceedings, (1984).
4. A. K. Likoded, S. R. Slabospitsky, "Nuclear Effects in Charmed Particle Hadronic Production, Serpukhov preprint 84-76 (1984).

Fig. 1: (a) Efficiency of the  $P_\mu > 9$  (GeV/c) and the  $P_\mu > 20$  (GeV/c) triggers as a function of the Feynman  $X_F$  of the  $D$  meson. Most semileptonic decays of  $D$  mesons with  $X_F > 0$  are detected by the  $P_\mu > 9$  (GeV/c) trigger. (b)  $dN_\mu/dP_\mu$  for prompt single muons per inelastic proton interaction. The solid curve is the expectation if  $D$  mesons are produced with a  $(1-X_F)^5$  distribution. (c) Sensitivity of  $\sigma_D(X_F > 0)$  to the assumed  $n$  if  $D$  mesons are produced with a  $(1-X_F)^n$  distribution. The extracted cross section is insensitive to charm production model assumptions.

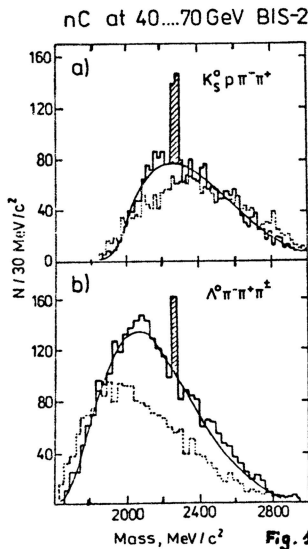


Hannelies Nowak  
 Institut fuer Hochenergiephysik der AdW der DDR  
 Berlin-Zeuthen, GDR

Although charmed particle production at SPS/FNAL and ISR energies has been studied by many experiments no information is available up to now at threshold energies. But this energy region corresponds to well defined low background conditions.

The subject of this talk is a study of  $\Lambda_c^+$  production by neutrons on Carbon and Hydrogen at 40-70 GeV. The experiment was performed with the BIS-2 spectrometer at the Serpukhov 70 GeV accelerator<sup>/4/</sup>.

During three running periods a total of  $11.4 \cdot 10^6$  triggers was recorded corresponding to  $6.0 \cdot 10^{11}$  incoming neutrons.



In fig.Ia the  $K_s^0 p \pi^+ \pi^-$  effective mass distribution (solid line) is presented. In fig.Ib is shown the  $\Lambda^0 \pi^+ \pi^+ \pi^-$  effective mass distribution (solid line). The mass values of both peaks are close to the mass of the charmed baryon  $\Lambda_c^+$ . Fitting a polynomial background to the data ( $130 \pm 18$ )  $K_s^0 p \pi^+ \pi^-$  and ( $57 \pm 14$ )  $\Lambda^0 \pi^+ \pi^+ \pi^-$  events are obtained corresponding to a  $10$

and 5 standard deviation effect, respectively. No significant peaks are seen in the charged conjugated effective mass distributions (dashed lines in fig.I).

Therefore we identify the observed peaks in fig.I with the Cabibbo favoured decays of the charmed baryon  $\Lambda_c^+$ <sup>/2/</sup>. Simulating  $\Lambda_c^+$  decays according to phase space including all experimental conditions it was found that only  $\Lambda_c^+$ 's with  $x_F > 0.5$  and  $p_T < 1$  GeV can be detected by the spectrometer corresponding to a momentum range of 40-70 GeV for the incident neutrons.

The following characteristic of the  $\Lambda_c^+$ 's are observed:

- I. The  $\Lambda_c^+$  production can be described by  $E d\sigma / d\vec{p} \sim \exp(-2.5 \pm 0.6) p_T \cdot (1 - x_F) (1.5 \pm 0.5)$

2. The results for  $\sigma \cdot B$  are  $(10^{+4}) / \text{ub}$  per Carbon nucleus for the  $\bar{K}^0 p \pi^+ \pi^-$  decay mode and  $(2.3 \pm 1.1) / \text{ub}$  per Carbon nucleus for the  $\Lambda^0 \pi^+ \pi^+ \pi^-$  decay mode leading to
3. a relative branching ratio of

$$\frac{\sigma \cdot B(\bar{K}^0 p \pi^+ \pi^-)}{\sigma \cdot B(\Lambda^0 \pi^+ \pi^+ \pi^-)} = 4.3 \pm 1.2$$

4. Using preliminary data on Hydrogen<sup>/3/</sup> an A-dependence of the cross-section of  $\alpha = 0.7 \pm 0.2 \pm 0.08$

was obtained including both statistical and systematic errors.

5. Using a branching ratio of 3.1% for the  $\Lambda^0 \pi^+ \pi^+ \pi^-$  decay mode and the A-dependence as obtained in this experiment a cross-section of  $13.4 / \text{ub/nucleon}$  for inclusive  $\Lambda_c^+$  production is estimated.

Moreover, we have studied an other property of the  $\Lambda_c^+$  - its polarization<sup>/4/</sup>. For both decay modes observed we have measured the decay asymmetry using the baryon or the kaon as a reference particle. The following asymmetries are obtained for the different reference particles:

Table  
 Measured asymmetry values

reference particle	value of asymmetry
p	$-0.22 \pm 0.13$
$K^0$	$0.21 \pm 0.13$
$\Lambda^0$	$0.34 \pm 0.26$

Like for the  $\Sigma^+$  hyperon the value of the  $\Lambda_c^+$  asymmetry parameter is different for different decay modes. In any case it is limited by  $|\epsilon| \leq 1$ .

Assuming a spin of  $\frac{1}{2}$  for the  $\Lambda_c^+$  the polarization equation leads to the inequality  $|\epsilon| \geq 2|A|$ . Averaging the measured asymmetry values for the reference baryons we obtain a lower limit for the  $\Lambda_c^+$  polarization

$$\epsilon \geq (50 \pm 25) \%$$

#### REFERENCES:

- /1/ Aleev A.N. et al, Yad.Fiz. 35, II75 (1982)
- /2/ Aleev A.N. et al, Z.Phys. C23, 333 (1984)
- /3/ Aleev A.N. et al, Paper 491 submitted to this conf.
- /4/ Aleev A.N. et al, Paper 492 subm. to this conf.

CHARM PARTICLE PRODUCTION AND DECAY PROPERTIES  
IN 360 GeV/c  $\pi^- p$  INTERACTIONS

J. Hrubec(\*)  
Institut für Hochenergiephysik

Vienna, Austria

The experimental set up of the NA27 experiment at the SPS (LEBC-EHS Collaboration) is briefly described in ref. 1 including a discussion of the improvements with respect to NA16. The results presented here correspond to the full statistics accumulated with the 360 GeV/c  $\pi^-$  beam (sensitivity =  $15.8 \pm .8$  events/ $\mu b$ ).

After the scanning for decay topologies and the subsequent measurements on a high precision machine the decays were analysed by kinematic fits. Strange particle decays are rejected and the particle identification system is used to solve the ambiguities in the interpretation. This procedure resulted in the selection of 118 interactions. For 71% of them both partners of the associated charm pair could be observed (202 decays).

Lifetimes, cross sections, branching ratios

The lifetimes are determined using the Maximum Likelihood Method. The cross sections are calculated only for the forward hemisphere ( $x_F > 0$ ).

$D^0, \bar{D}^0$ : Their decays into 4 charged particles (V4 topology) can be considered as a clean sample without background. 22 V4 decays have been observed and 16 out of them are kinematically identified as decays of neutral D-mesons:

$$\tau = 3.5 \pm 1.4 \times 10^{-13} \text{ s (based on 11 decays)}$$

$$\sigma = (10.3 \pm 3.5) \mu b \quad (x_F > 0)$$

$$\text{BR}(D^0, \bar{D}^0 \rightarrow K^+ \pi^+ \pi^-) = (7.1 \pm 2.5)\%$$

The sample of V2 decays often leads to kinematically ambiguous solutions due to the missing neutral particles. Nevertheless, the results for the lifetime and cross section are compatible with these quoted above, confirming the quality of these data. The semi-electronic branching ratio could be determined:

$$\text{BR}(D^0, \bar{D}^0 \rightarrow e^\pm + X) = 7 \pm 6 \%$$

$D^+, \bar{D}^-$ : 60 decays of charged charm particles are observed as vertices with 3 or 5 outgoing charged tracks (C3, C5 topology). Out of these 33 are identified by kinematics as decays of charged D's:

$$\tau = 9.8 \pm 4.4 \times 10^{-13} \text{ s (based on 14 decays)}$$

$$\sigma = (6.7 \pm 2.7) \mu b \quad (x_F > 0)$$

The resulting ratio of the lifetimes is therefore:

$$\frac{\tau(D^+, \bar{D}^-)}{\tau(D^0, \bar{D}^0)} = 2.8 \pm 2.4$$

Some of the identified  $D^0$  ( $\bar{D}^0$ ) could come from decays of  $D^*$ 's. This might account for the higher cross section of the neutral D's.

$F^+, \bar{F}^-$ : Since no decay could be uniquely interpreted as F meson only an upper limit for the following ratio can be given:

$$\frac{\sigma_F \cdot \text{BR}(F^+ \rightarrow C3, C5)}{\sigma_D \cdot \text{BR}(D^+ \rightarrow C3, C5)} \leq 12\% \text{ (90\% CL)}$$

assuming  $\tau(F) = 3.2 \times 10^{-13} \text{ s (ref. 2)}$ .

$\Lambda_c, \bar{\Lambda}_c$ : 4 decays are identified in different channels ( $\Sigma^+ \pi^-, \Lambda_c^0 \pi^+ \pi^-, K^+ p \pi^-, K^- p \pi^+$ ), in 2 events the associated partner is a well established D:

$$\tau = 1.0 \pm 0.9 \times 10^{-13} \text{ s}$$

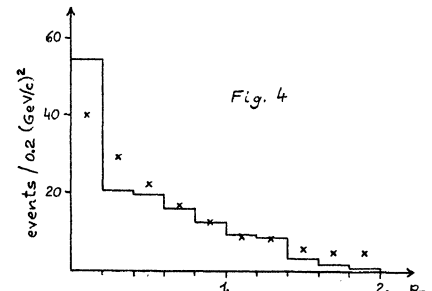
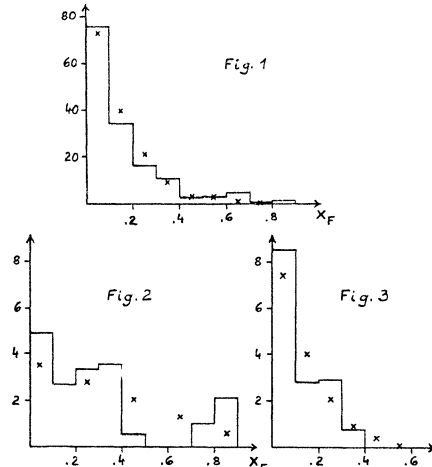
Under simple assumptions for the branching ratios for the  $D'$ , F and  $\Lambda_c$  the following upper limits (90% CL) can be determined for the cross sections:

$$\sigma(F) \leq 1 \mu b \quad \text{and} \quad \sigma(\Lambda_c) \leq 4 \mu b$$

This leads to a preliminary estimate for the inclusive total charm cross section in the forward hemisphere:

$$17 \mu b \leq \sigma_{\text{tot}}(\text{charm}) \leq 22 \mu b \text{ (90\% CL).}$$

$\frac{X_F \cdot p_T^2}{\sigma}$ : The figures 1, 2 and 3 show the weighted  $X_F$  distributions for ( $D^0$  and  $\bar{D}^0$ ),  $D^-$  and  $D^+$  respectively. The distribution for the  $D^-$  extends to much higher  $X_F$  values than for the  $D^+$ . This could be interpreted as the effect of a leading quark from the incident  $\pi^-$ . Fig. 4 displays the weighted  $p_T^2$  distribution for all D's.



Figs 1, 2, 3 and 4

(\*) Presently at CERN, Geneva, Switzerland

The crosses in fig. 1, 3 and 4 indicate the curves predicted by a fusion model. For fig. 2 the crosses correspond to  $f(X_F) \propto (1 - X_F)^{-1}$ .

#### Pair correlations

16 pairs of  $(D\bar{D})$  have been reconstructed with  $X_F > 0$  for the pair. Fig. 5 shows the weighted effective mass spectrum of the  $(D\bar{D})$  system which peaks around  $4 \text{ GeV}/c^2$ . The prediction of a fusion model (taking into account the intrinsic  $k_T$  of the colliding constituents and the  $D^*$  production) is overlayed to the experimental distribution.

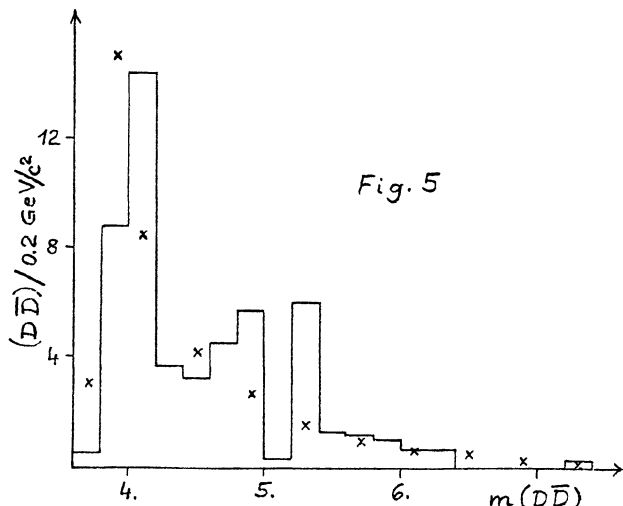


Fig. 5

#### Future prospects

It will be interesting to compare these results with the data already taken with protons of  $400 \text{ GeV}/c$  incident momentum. A further step is an analogous experiment with a proton beam of about  $1 \text{ TeV}/c$ , which is already approved at FNAL.

#### REFERENCES:

- [1] M. Aguilar-Benitez et al., Neutral D meson properties in  $360 \text{ GeV}/c \pi^- p$  interactions, CERN/EP 84-73 (1984), submitted to Phys. Lett. B.
- [2] R. Bailey et al. (ACCMOR Collaboration), Measurement of mass and lifetime of hadronically produced charmed F mesons, Phys. Lett. 139B (1984) 320.

# HADROPRODUCTION OF CHARM

TAVERNIER, Stefaan  
Inter-University Institute for High Energies  
Vrije Universiteit Brussel  
Brussels, Belgium

## 1. INTRODUCTION

In this review I mainly consider open charm production. Total cross sections atomic number dependence and  $x_F$  dependence are discussed. Several results concerning these topics were presented at this conference, but some new results not submitted here are also included. A presentation of the holographic bubble chamber experiment NA-25 is given in an appendix because this experiment has presented new data and is not discussed elsewhere in these proceedings.

## 2. TOTAL CHARM PRODUCTION CROSS SECTIONS IN PROTON-PROTON INTERACTIONS

Figure 1 presents a compilation of total charm production cross sections in pp or pn interactions as a function of  $\sqrt{s}$ . The data are taken from references [1] to [20].

At ISR energies ( $\sqrt{s} \sim 60$  GeV) there is a long standing problem that results based on exclusive hadronic final states suggest cross sections of  $\sim 1$  mb while results based on the observation of leptons suggest  $\sigma \sim 100 \mu\text{b}$ . The most convincing evidence for large cross sections comes from the two SFM experiments [18] and [19]. The latter had already revised his cross sections with a factor 2 downward at the Brighton Conference in 1983. Here in Leipzig we learned of new branching ratio's for  $D^0 \rightarrow K^-\pi^+$  and  $D^+ \rightarrow K^-\pi^+$  from Mark III [21] which are a factor two bigger than the particle data group values. As a result the cross section for both SFM experiments should be devided by 2 and these revised values are displayed in fig.1. The conflict between both sets of data has not disappeared but is nevertheless much reduced. A value of  $\sigma \sim 200-300 \mu\text{b}$  for the charm cross sections now seems a reasonable guess. This value is no longer in conflict with the inclusive electron spectra [19], but is still difficult to reconcile with the dilepton cross sections [13, 14, 15]. Two experiments, the Axial Field Spectrometer and one of the SFM experiments have taken more data which are not yet analysed and which possibility will shed light on this question. For completeness I also mention a cosmic ray emulsion experiment [20] which finds  $\sigma \sim 1$  mb at  $\sim 10$  TeV incident momentum.

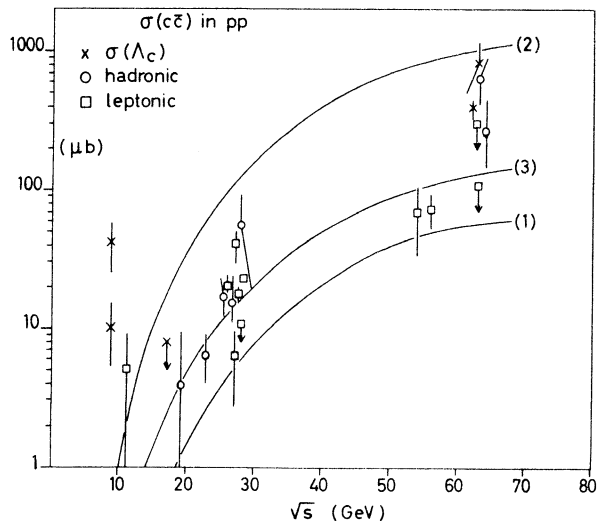


Fig. 1 : Total charm pair production cross sections in pp or pn interactions. The curves are model calculations : (1) charm creation, Combridge [24] with  $m_c = 1.3$  GeV; (2) charm excitation, Combridge [24] with  $m_c = 1.3$  GeV and  $Q_o^2 = m_c^2/2$ ; (3) charm excitation, Odorico [26] with  $m_c = 1.5$  GeV/c and  $Q_o^2 = m_c^2/2$ .

At  $\sqrt{s} \sim 26$ , many measurements were made with widely different techniques. There is a fair agreement between the different experiments if a linear A dependence is assumed for the charm cross section. I would like to single out four experiments : EHS [7] with  $A = 1$ , the holographic bubble chamber [4] with  $A = 17$ , the FNAL-muon beam dump [6] with  $A = 56$ , and the FNAL-neutrino beam dump [11] with  $A = 184$ , which are all compatible with  $\sigma \sim 20 \mu\text{b}$ . If we assume  $A^{\alpha_{c\bar{c}}}$ ,  $\alpha_{c\bar{c}} = 0.72$ , the data on nuclear targets are multiplied by 2.2, 3.1 and 4.3 respectively. This would completely spoil the agreement between the different experiments. I conclude that these experiments taken together very strongly favour  $\alpha_{c\bar{c}} \approx 1$ . To obtain a quantitative estimate of  $\alpha_{c\bar{c}}$  I have fitted all the data points between 200 and 400 GeV/c with a cross section which depends linearly on the beam momentum. The result of the 3 parameter fit is  $\alpha_{c\bar{c}} = 1.09 \pm 0.12$ .

In this context I must mention the result from [11] where the prompt neutrino flux was measured on Berillium and Tungsten and the authors derive

$\alpha_{c\bar{c}} = 0.74 \pm 0.07$ . This result however is valid only for charm production averaged over their acceptance, which means that it applies to charm produced at  $x_F \sim 0.5$ . The same comment applies to [1] which claims  $\alpha_{c\bar{c}} \sim 0.7 \pm 0.2 \pm 0.08$ . The solution of this apparent contradiction is that  $\alpha_{c\bar{c}}$  is probably a function of  $x_F$ . Figure 2 compiles data for various inclusive particle production cross sections in pp as a function  $x_F$  [22]. The total inelastic cross section for pp interactions has  $\alpha = 0.72$  [23] while figure 2 shows that  $\alpha(x_F = 0.5) \approx 0.53$  for the production of "ordinary" hadrons. A similar behaviour could apply to charm production. If the above assumption is correct we should observe that the coefficient  $n$  in the  $(1-x_F)^n$  dependence of the cross section is higher if measured on heavy nuclei. If we compare H<sub>2</sub> and Fe we should approximately have  $n_{Fe} = N_{H_2} + 1.6$ . It is interesting to see that the data indeed support such a behaviour. Using results on hydrogen, iron and tungsten [7, 6, 11], we find  $n = 1.8 \pm 0.8$  (H<sub>2</sub>);  $n = 5 \pm 0.8$  (Fe) and  $n = 3.2 \pm 0.2 \pm 0.4$  (W). For the hydrogen data however the non invariant cross section  $d\sigma/dx_F$  was fitted while the Fe and W data used the invariant cross section  $E d\sigma/dx_F$ . If the H<sub>2</sub> data were also fitted with the invariant cross section, the exponent  $n$  would be even lower. Also, the results from the nuclear targets do not distinguish D and  $\Lambda_c$  production, and probably have some  $\Lambda_c$  included in their charmed particles, while the H<sub>2</sub> experiment only uses fitted D mesons. These two remarks reinforce the conclusion that the exponent  $n$  is larger on nuclear targets than on hydrogen.

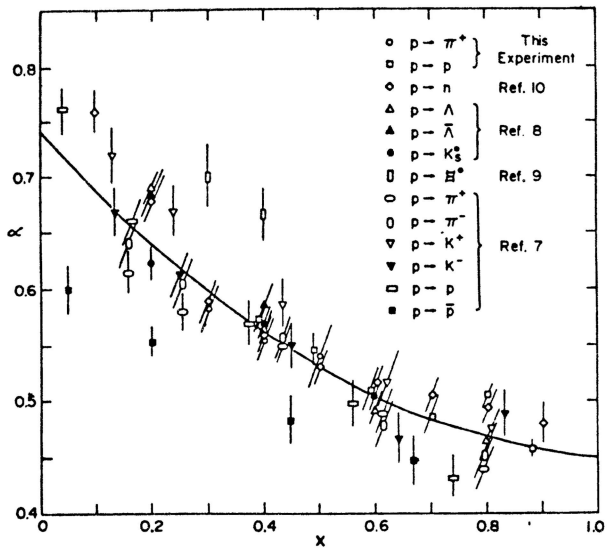


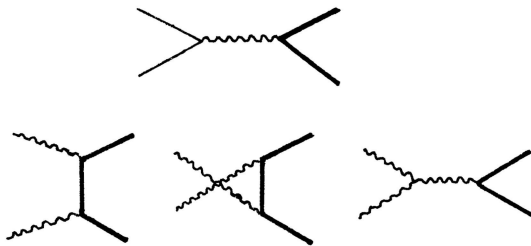
Fig. 2 : Variation of the atomic number dependence parameter  $\alpha$  with  $x$  for various particles produced by protons at a transverse momentum of 300 MeV/c and for incident energies from 24 to 400 GeV. The curve is a polynomial fit to the data. Figure from [22].

Turning now to cross sections below  $\sqrt{s} \approx 26$  GeV/c we see some conflicting results. The holographic bubble chamber experiment [4] has measured the charm cross section with the same technique at 200 and 360 GeV/c and suggests a cross section which decreases rapidly with energy, while the Bis-2 collaboration [1] finds a very large cross section at  $\sqrt{s} \approx 8.7$  GeV. Assuming all  $\Lambda_c$  are produced at  $|x_F| > 0.5$  they find  $\sigma(\Lambda_c) = 42 \pm 16 \mu b$  ( $K^0 p \pi^+ \pi^-$ ) or  $\sigma(\Lambda_c) = 10 \pm 5 \mu b$  ( $\Lambda^0 \pi^+ \pi^+ \pi^-$ ). Admittedly the branching ratio's of the  $\Lambda_c$  are not very well known, but these results definitely suggest a surprisingly large cross section. The data, if they are to be taken seriously would imply a charm cross section which is almost constant below  $\sqrt{s} \approx 26$  GeV/c!!! In this case we would have to assume that at  $\sqrt{s} \approx 10$  nearly all charm is produced in  $(\bar{D}\Lambda_c)$  final states, while with increasing energy ( $D\bar{D}$ ) production would rapidly become more important. The rapid increase of the cross section observed in the holographic bubble chamber could than be explained by the fact that the visibility of the short lived  $\Lambda_c$  in the bubble chamber is poor if the lifetime is only  $\sim 10^{-13}$  s, and what is observed is basically the rise in ( $D\bar{D}$ ) cross section.

It is certainly necessary to have this confirmed before we can take it seriously.

### 3. MODEL CALCULATIONS

My discussion of model calculation for the total charm production cross sections will be very brief and not attempt will be made to be complete. The most straightforward model for charm production is a QCD calculation assuming charm is created either in the fusion of two gluons or in the annihilation of a charm-anticharm pair by the diagrams given below.



This mechanism is referred to as "charm creation". Curve (1) on fig. 1 is such a calculation taken from Combridge [24] with the charmed quark mass  $m_c = 1.3$  GeV.

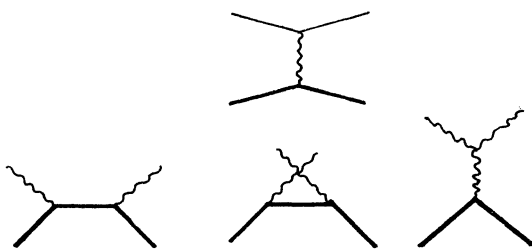
The result falls short of the observed cross section by about a factor 3. One can wonder whether the uncertainties in this calculation, namely the charmed quark mass  $m_c$ , the higher order corrections, and the gluon distribution functions in the proton, are not sufficient to explain such a difference. Another argument against the charm creation mechanism

is that charmed particles produced in this way are very centrally produced, having a distribution like  $(1-x)^n$ ,  $n \approx 7$ .

This result is obtained even if we assume that the charmed particle inherits all the momentum of the charmed quark. A glimmer of an escape route exists if one assumes a recombination mechanisms where the charmed particle acquires its momentum from one of the initial valence quarks. In  $p\bar{p}$  interactions only the  $\bar{D}$  meson can acquire a harder  $x_F$  distribution in this way, and the  $D$  meson must be centrally produced. In EHS however [7] no difference is observed between the  $x_F$  distributions for the  $D$  and the  $\bar{D}$  and both are compatible with  $(1-x)^n$ ,  $n = 1.8$ . This results seems fatal for the charm creation models. However the EHS results is based on a very small statistics and it is essential that this result be confirmed with the data from the new run. An additional problem is that some  $D$  mesons might result from  $\Lambda_c^*$  decay. In this case we can have two components in the  $x_F$  distribution of the  $D$  mesons : a very central component from the directly produced  $D$  mesons and a harder component for the  $D$  mesons from  $\Lambda_c^*$  decay. It should also be mentionned that for  $\pi^-$  induced charm production EHS finds that  $D^0$  and  $D^-$  mesons (which can not contain a valence quark) in the forward direction are indeed produced centrally with  $n \approx 5$ . This makes it only more essential to confirm the different situation in  $p\bar{p}$  reactions.

In conclusion, the charm creation models have some real difficulties in describing the data, but it is not clear to me that they are completely ruled out.

If not enough charm can be created in the collision it must somehow be present in the hadron before the interaction. Two classes of models exist which incorporate this idea. Charm excitation is advocated by e.g. Combridge [24] or Odorico [26]. It assumes that the charm which is present as "charm sea" in the hadron gets "excited" by the interaction. The relevant diagrams are given below :



It may seem that the smallness of the charm content in the sea of the nucleon would make this contribution negligible, but the cross sections corresponding to the diagrams above diverge as  $Q^2 \rightarrow 0$ . The charm content of the nucleon also vanishes at

$Q^2 \rightarrow 0$  so that the result is finite. In the actual calculations one assumes an essentially arbitrary cutoff parameter  $Q_0^2$  below which the charm content of the proton is zero. At larger  $Q^2$  the charm sea is generated perturbatively according to the QCD evolution prescriptions. The result of this is that the value of the cross section obtained has very large uncertainties. It remains that, with natural choices of the parameters in the calculation, it is possible to obtain cross sections from charm excitation which are much larger than the ones from charm creation. Curves (2) and (3) on figure 1 show the result of calculations along this lines by two different authors [24, 26].

The other model is the intrinsic charm model [27]. The basic idea is that the proton contains higher Fock states which contain a  $c\bar{c}$  pair. In this case the charmed quarks carry a large fraction of the momentum of the hadron. The most characteristic prediction of this model is that charmed particles, even those that can not recombine with one of the valence quarks of the initial hadron, should be produced at rather large  $x_F$ .

Charm excitation or intrinsic charm are not meant to replace charm creation. The basic process of charm creation generated by the QCD diagrams given above must exist. Rather, there may be other contributions which at least at certain energies and for certain incident particles may dominate over charm creation. There is no reason to assume that the same mechanism will dominate everywhere.

#### 4. CROSS SECTIONS FOR $\pi^-$ INDUCED CHARM PRODUCTION

Data on this subject are compiled in fig. 3 and compared with  $p\bar{p}$  data in the same energy range. There is a clear need for better data before a real conclusion can be drawn. Nevertheless, to the bewiling eye, figure 3 suggests a cross section for charm in  $\pi^-$  induced reactions which is larger at lower energies, rises less fast and becomes equal to the charm cross section in  $p\bar{p}$  at 400 GeV/c. Such a behaviour is observed for  $\psi$  production [28]. In charm creation models it occurs naturally and is due to the fact that in  $\pi^- p$  at low energy the  $q\bar{q}$  annihilation diagram dominates, while at higher energies the gluon fusion diagrams dominate for all incident hadrons.

#### 5. PROBLEMS AND OUTLOOK

As the reader has certainly realised during these few pages, our knowledge of open charm production in hadron-hadron interactions is still unsatisfactory. There are conflicting data on the cross sections at ISR energies ( $\sqrt{s} = 60$  GeV) and at low energies ( $\sqrt{s} \approx 10$  GeV), and no clear winner emerges.

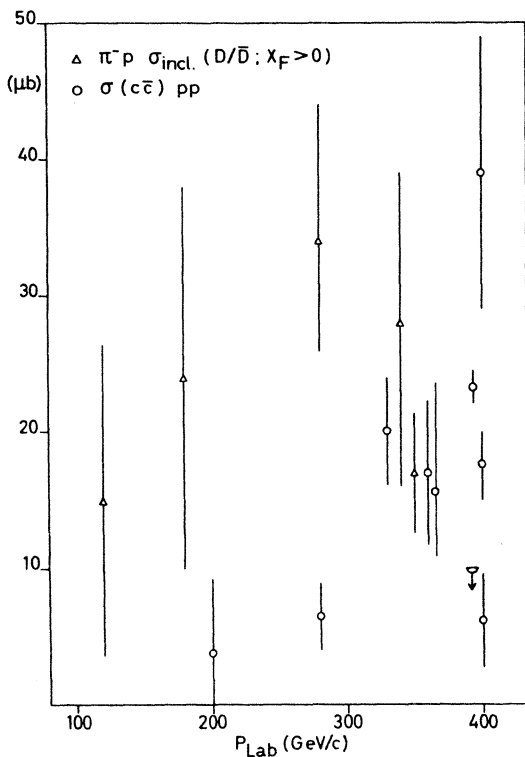


Fig. 3 : Total charm pair production cross sections in  $\pi^-$  induced and proton induced reactions. For pions the quantity plotted is the inclusive  $D/\bar{D}$  production  $\sigma$  for  $x_F \rightarrow 0$ .

The question of the relative importance of  $D\bar{D}$  and  $\bar{D}\Lambda_c^0$  is essentially open. The answer to the basic question concerning the dominant production mechanism remains uncertain. Predicting charm cross sections at future collider energies, a matter of considerable practical importance, is hazardous.

The recent observation of  $D^*$  at the CERN collider ( $\sqrt{s} = 540$  GeV) [30] is not particularly helpful in this respect since it concerns charm production in the fragmentation of gluon jets, presumably a different production mechanism, responsible for a small part of the total charm production cross section only. For the related question of bottom production in hadron-hadron interactions, no convincing signal has been observed so far. Only one new (negative!) result concerning  $B$  production was presented at this conference [29]. From the observed number of like sign muons these authors derive an upper limit (90% C.L.) on  $\sigma(B\bar{B})$  of less than 10-50 nb in pp interactions at 400 GeV/c. The range of values corresponds to different production models to calculate the acceptance. The same collaboration has published a limit of 2-10 nb for  $\sigma(B\bar{B})$  in  $\pi^- p$  at 280 GeV/c [31].

#### APPENDIX

A MEASUREMENT OF THE TOTAL CHARM PRODUCTION CROSS SECTION IN pp INTERACTIONS AT 200 AND 360 GeV/c USING

#### THE HOLOGRAPHIC BUBBLE CHAMBER HOBC.

Experiment NA25 : Bari, Brussels, CERN UCL, Mons, Paris VI, Strasbourg, Vienna collaboration

The experimental set up consists of a holographic heavy liquid bubble chamber HOBC and a muon trigger. It is described elsewhere [32]. The active liquid in the bubble chamber is  $C_3F_8$  ( $\langle A \rangle \approx 17$ ). Thanks to holography, bubbles of  $10 \mu\text{m}$  are recorded with a depth of field of several cm. Immediately behind the bubble chamber is a massive iron and tungsten dump. Picture taking is triggered by a muon of  $> 6$  GeV/c. The charge or the momentum of the muon is not determined.

The holograms are carefully scanned for any secondary activity in a 2.4 mm wide band extending forward from the vertex to the end of the chamber. A secondary activity is considered a decay candidate if there is no backward or heavily ionising track. Gamma conversions and delta electrons are recognised by multiple scattering. Charm decay candidates are required to satisfy suitable cuts on transverse decay distance and impact parameter of the decay track relative to the primary vertex. These cuts are chosen such that only a few percent of the charm decays are removed. In addition it is necessary to require cuts on projected opening angles or decay angles to remove  $\gamma$ -conversions or  $\delta$ -electrons where a small amount of multiple scattering could simulate a decay with a very small decay angle.

To reduce the background further we restrict our attention to the sample with two charm decay candidates in the same event. In this sample the background can be evaluated under the assumption that the probability that a secondary interaction simulates a charm decay candidate is independent of the fact that there is already such a decay present in the event. We observe 16 events at 360 GeV/c (background 3.85) and 3 events at 200 GeV (background 1.70).

To convert these numbers into cross sections two important weight factors have to be applied. The effect of the various scanning cuts is evaluated with a detailed Monte Carlo program and the corresponding weight is 1.64 per decay. The visibility weight is determined from a comparison of the experimentally observed length distribution of the charm decays with the expected distribution from the Monte Carlo calculation. The visibility is then parametrised as a function of the distance by

$$V = V_\infty (1 - e^{-\beta L})$$

$V_\infty$  is the scanning efficiency at large distance and it is determined as usual from two independent scans and is found to be 95% after two scans. The visibility weight determined by the above procedure is

$1.54^{+0.38}_{-0.29}$  per decay. Assuming linear A dependence and an average semileptonic branching ratio of 8% the cross sections becomes :  $17^{+5.5}_{-5.1} \mu\text{b}$  and  $3.9 \pm 5.5 \mu\text{b}$  at 360 and 200 GeV/c respectively.

#### REFERENCES

1. A.N. Aleev et al., Results from the Bis-2 collaboration presented at this conference by H. Nowak; A.N. Aleev et al., Sov.J.Nucl.Phys. 37 (1983) 877
2. A.E. Asratyan et al., Phys. Lett. 79B (1978) 497
3. R. Bailey et al., Nucl.Phys. B239 (1984) 15
4. M. Muccia et al., A measurement of the total charm production cross section in pp interactions at 200 and 360 GeV/c; Results presented at this conference, see appendix. See also Brussels intern rapport IIHE-84.03.
5. Liang Tzeng, Measurement of the hadronic charm production cross section in a high resolution streamer chamber experiment; Thesis, Yale University, April 1984, Publication in preparation.
6. J.L. Ritchie et al., Phys.Lett.126B (1983) 499  
J.L. Ritchie et al., Phys.Lett.138B (1984) 213  
Results from the E-595 experiment, presented at this conference by A. Bodek
7. M.Aguilar-Benitez et al.Phys.Lett.123B(1983)103  
M.Aguilar-Benitez et al.Phys.Lett.122B(1983)312  
M.Aguilar-Benitez et al.Phys.Lett.123B(1983)98  
M.Aguilar-Benitez et al.Phys.Lett.135B(1984)237  
M.Aguilar-Benitez et al., Neutral D-meson properties in 360 GeV/c  $\pi^- p$  interactions, submitted to Physics Letters; Results from NA27 on charm production in  $\pi^- p$  interactions, Presented at this conference by J. Hrubec
8. H.Abramowicz et al.,Zeit.Phys.C,13 (1982) 13
9. H. Wachsmuth, Results from the BEBC beam dump experiment, Results presented at this conference  
P. Fritze et al., Phys. Lett. 96B (1980) 427
10. M. Jonker et al., Phys. Lett. 96B (1980) 435 and statement by F. Niedergall during the discussion at this conference
11. R. Loveless, Results from the FNAL  $\nu$ -beam dump experiment E-613, Presented at the Lund conference on Multiparticle Dynamics, 1984;  
B. Roe, New results from the Fermilab prompt neutrino experiment, Proceedings of the Brighton Conference, Brighton, July 1983, page 318;  
R.C. Ball, Phys.Rev.Lett. 51 (1983) 743
12. T. Aziz et al., Nucl.Phys. B199 (1982) 424  
T. Aziz et al., Neutral charm production in 400 GeV/c proton emulsion interactions,TIFR-BC-84-3
13. H.G. Fischer and W.M. Geist, Zeit.Phys.C 19 (1983) 159
14. A.G. Clark et al., Phys.Lett.77B (1978) 339
15. A. Chilingarov et al., Phys. Lett.83B (1979) 136 and reference therein
16. W. Lockmann et al., Phys.Lett.85B (1979) 443
17. J. Irion et al., Phys.Lett.99B (1981) 495
18. M. Basile et al., Nuovo Cimento 63A (1981) 230  
M. Basile et al., Nuovo Cimento 65A (1981) 457  
M. Basile et al., Nuovo Cimento 67A (1981) 40  
M. Basile et al., Lett.Nuovo Cimento 33 (1982)3  
M. Basile et al., Lett.Nuovo Cimento 33 (1982) 17
19. D. Drijard et al., Results on charm production, Proceedings of the High Energy Physics Conference, Brighton (UK), july 1983, page 308
20. H. Fuchi et al., X-Particle Search in Super High Energy Interactions, 16th International Cosmic Ray Conference, Kyoto 1979, Volume 6, page 112.
21. The properties of charmed D mesons measured in  $e^+ e^-$  collisions at  $\sqrt{s} = 3,768$  GeV, Mark III collaboration, Results presented at the Leipzig conference by R. Schindler
22. D.S. Barton et al., Phys. Rev.D27 (1983) 2580
23. A.S. Carroll et al., Phys. Lett.80B (1979) 319
24. B.L. Combridge, Nucl.Phys.B151 (1979) 429
25. R.Winder and C.Michael,Nucl.Phys.B173 (1980) 59
26. R. Odorico, Flavour exitation of open charm, Proceedings of the Moriond workshop on new flavours, Les Arcs 1982
27. S.J. Brodsky et al., Phys. Lett. 93B (1980) 451  
S.J. Brodsky et al., Phys. Rev. D23 (1981) 2745
28. M.J. Corden et al., Phys. Lett. 68B (1977) 96  
J. Badier et al., Zeit.Phys. C20 (1983) 101
29. J. Badier et al., Paper presented at this conference by J. Karyotakis
30. G. Arnison et al.,  $D^*$  production at the SPS collider, Submitted to Physics Letters B, Submitted to this conference
31. J. Badier et al., Phys. Lett. 124B (1983) 535
32. A. Hervé et al., Nucl.Instr.Meth. 202 (1982) 412  
J.L. Benichou et al., Nucl. Instr. Meth. 214 (1983) 245;  
S.P.K. Tavernier, Holographic image recording in visual particle detectors, Proceedings of the 2nd Pisa Conference on New Particle Detectors (1983), To be published in Nucl. Instr. Meth.  
M. Barth et al., A scanning table for holographic bubble chamber or streamer chamber images; to be published in Nucl. Instr. Meth.